

Capacity Maximization with Polarization-Agile Antennas in the MIMO Communication System

Seok-Chul Kwon[†], Member, IEEE and Andreas F. Molisch, Fellow, IEEE

Department of Electrical Engineering, University of Southern California

[†]Next Generation and Standards Division, Intel Communication and Devices Group

Email: [†]seok.chul.kwon@intel.com, molisch@usc.edu

Abstract—Polarization diversity is an important candidate for improving the channel capacity in multiple-input multiple-output (MIMO) communication systems. The use of polarization-agile antennas enables to reap important benefits of polarization diversity without the need for additional up/down-conversion chains and their associated cost and energy consumption. In this paper we propose a novel scheme of *polarization pre-post coding* based on the theoretical (approximate) closed-form derivation of *optimal transmit/receive polarization vectors* to maximize channel capacity when polarization agility is available only at one link end. We use those as basis for an *iterative joint polarization pre-post coding* for polarization agility at both link ends. Simulations validate that the obtained capacity is in a close agreement with that obtained by exhaustive numerical search for optimal transmit/receive polarization orientation. Utilizing our scheme of joint polarization pre-post coding improves system performance by 3 dB to 5 dB in terms of the SNR.

I. INTRODUCTION

The phenomenon of channel depolarization in wireless communication systems has long been attracting substantial attention since it is the key to utilizing polarization diversity, see, e.g., [1]–[6]. Wireless communication systems with multi-polarized antennas utilize polarization diversity to increase channel capacity and reduce bit/symbol error rate [4], [7]–[12]. In other words, the unique characteristics of polarized wireless channels can remarkably improve the performance of the MIMO system beyond that of the conventional system not fully utilizing polarized-channel characteristics.

Much of the existing literature on polarization diversity assumes that the transmitter (Tx) and receiver (Rx) have collocated (mounted) *dual-polarized* antennas, such that two antenna ports are available for each spatial position. Compared to the case where the same number of antennas, but only a single polarization per antenna is available, this obviously leads to an increase in diversity and capacity, although this gain depends significantly on the cross-polarization discrimination (XPD) [9]. However, the collocated dual-polarized antenna requires doubling the number of antenna ports, with the associated increase in the number of RF (up/down-conversion) chains and increased baseband processing. Hence, for the fairness in comparing the performance of the MIMO system, we consider the antenna array structure that has the same total number of antenna ports in this paper. That is, we take into account spatially separated antennas at the Tx and Rx, each of which has one antenna port and polarization, whether the polarization is fixed or reconfigurable.

For the case of dual-polarized antennas, a number of important insights have been achieved by previous works, see, e.g., [4], [7], [11], [12]. In recent years, polarization-agile antennas have emerged, which can adapt their transmit/receive polarization (Tx/Rx-polarization) while having only a single output port [13], [14]. In this paper we propose and analyze a MIMO communication system with such polarization-agile antenna elements and the functionality of polarization precoding/postcoding, which we call “*polarized-MIMO*” (*P-MIMO*) in this paper. Hence, the implementation of the P-MIMO system is feasible by utilizing aforementioned polarization-agile antennas. The main contributions of this paper can be summarized as follows:

- we introduce the P-MIMO communication system, which utilizes polarization precoding and postcoding at polarization-agile antennas;
- we provide a closed-form approximation of the optimal Tx/Rx-polarization vectors in a system with polarization agility at one link end to achieve channel capacity that is greater than that of a conventional MIMO communication system (with the same number of ports) with fixed single- or multi-polarized antennas;
- we validate by simulations that the P-MIMO channel capacity corresponding to the closed-form approximation of the optimal Tx/Rx-polarization vectors is in a close agreement with the maximum capacity obtained by the brute-force numerical search;
- we propose an iterative joint polarization pre-post coding to achieve global optimal Tx/Rx-polarization vectors in systems with polarization agility at both link ends.

The remainder of this paper is as follows. Section II presents the P-MIMO system model focusing on polarization-agile antennas. In Section III, the polarization precoding/postcoding scheme utilizing optimal Tx/Rx-polarization vectors is proposed and described in detail. The validation of the proposed polarization precoding/postcoding scheme is provided via comparing theoretical and numerical results in Section IV. Finally, Section V concludes the paper with the summary.

II. SYSTEM MODEL

Figure 1 shows the block diagram of the system we consider. Both the Tx and the Rx have multiple antenna elements (N_t and N_r of them, respectively). Each antenna element is polarization-agile, i.e., its polarization vector $\vec{p}_{Tx,j}$ (or $\vec{p}_{Rx,i}$),

with $j \in \{1, \dots, N_t\}$ ($i \in \{1, \dots, N_r\}$) is adjusted by the Tx (Rx) according to the channel state information (CSI). We assume that perfect CSI at all antenna elements is available at the Rx (CSIR) as well as the Tx (CSIT). Note that the CSI is available for both orthogonal polarization directions; it can be obtained through training schemes similar to those employed in antenna selection systems (see, e.g., [15]). The impact of imperfect CSI is outside the scope of this paper and will be analyzed in future work.

In addition to the polarization precoding/postcoding, the P-MIMO system contains precoding/postcoding that allows optimum exploitation of the spatial degree of freedom; it is well-known from conventional (non-polarization-agile) spatial multiplexing systems with perfect CSI [16] that linear precoding/postcoding based on the singular value decomposition (SVD) of the effective channel matrix maximizes channel capacity. It is intuitive that exploiting polarization-agile antenna elements with polarization precoding/postcoding - on top of the standard SVD-based spatial precoding/postcoding - can achieve higher capacity than single-polarization or fixed-polarization antenna elements (with the same number of data streams or RF up/down-conversion chains). Mathematical derivations for this intuition will be presented below.

The effective channel impulse response matrix in Fig. 1 can be expressed as

$$H^{\text{eff}} = \begin{bmatrix} \vec{p}_{\text{Rx},1}^T H_{11} \vec{p}_{\text{Tx},1} & \cdots & \vec{p}_{\text{Rx},1}^T H_{1N_t} \vec{p}_{\text{Tx},N_t} \\ \vdots & \ddots & \vdots \\ \vec{p}_{\text{Rx},N_r}^T H_{N_r,1} \vec{p}_{\text{Tx},1} & \cdots & \vec{p}_{\text{Rx},N_r}^T H_{N_r,N_t} \vec{p}_{\text{Tx},N_t} \end{bmatrix}, \quad (1)$$

where the operation $(\cdot)^T$ is the transpose of a given vector or matrix, and the dimension of H^{eff} is $N_r \times N_t$. Further, H_{ij} is called ‘‘polarization-basis matrix’’ in our paper, which is expressed as

$$H_{ij} = \begin{bmatrix} h_{ij}^{\text{vv}} & h_{ij}^{\text{vh}} \\ h_{ij}^{\text{hv}} & h_{ij}^{\text{hh}} \end{bmatrix}, \quad (2)$$

where h_{ij}^{xy} with $x \in \{v, h\}$; $y \in \{v, h\}$ is the XY-channel impulse response from the Y-polarization Tx antenna to the X-polarization Rx antenna. For example, h_{ij}^{hv} is the HV-channel impulse response from the vertically polarized (V-polarization) Tx antenna to the horizontally polarized (H-polarization) Rx antenna. Lastly, $\vec{p}_{\text{Tx},j}$ and $\vec{p}_{\text{Rx},i}$ are, respectively, the Tx-polarization vector at the j th Tx antenna and the Rx-polarization vector at the i th Rx antenna, and they are expressed as

$$\vec{p}_{\text{Tx},j} = \begin{bmatrix} p_{\text{Tx},j}^{\text{v}} \\ p_{\text{Tx},j}^{\text{h}} \end{bmatrix} = \begin{bmatrix} \cos \theta_j \\ \sin \theta_j \end{bmatrix}, \quad (3)$$

$$\vec{p}_{\text{Rx},i} = \begin{bmatrix} p_{\text{Rx},i}^{\text{v}} \\ p_{\text{Rx},i}^{\text{h}} \end{bmatrix} = \begin{bmatrix} \cos \theta_i \\ \sin \theta_i \end{bmatrix}. \quad (4)$$

Here, we call the angles θ_j and θ_i Tx- and Rx-polarization angles, respectively. It is worth mentioning that Tx- and Rx-polarization vectors are unit vectors so that the overall signal power is preserved after polarization precoding and postcoding.

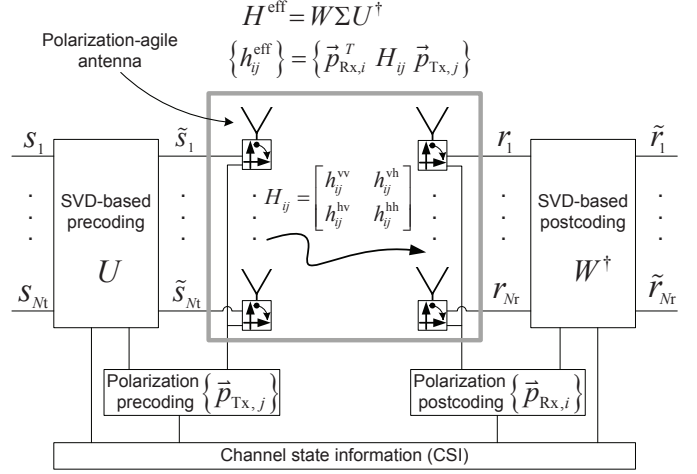


Fig. 1. MIMO system with polarization-agile antenna.

III. POLARIZATION PRE-POST CODING AT THE POLARIZATION-AGILE ANTENNA

A. Polarization Precoding and Postcoding with Optimal Tx- and Rx-polarization

The Tx and the Rx can utilize SVD-based precoding and postcoding under the assumption of full CSIT along with the full CSIR. The combination of SVD-based precoding and postcoding achieves the MIMO channel capacity for a given channel matrix via constructing the structure of parallel channels [16]. On the other hand, the MIMO communication system with polarization-agile antennas in Fig. 1 can perform tuning of the effective channel impulse response matrix H^{eff} itself in (1) by either polarization precoding at the Tx or polarization postcoding at the Rx; or joint polarization pre-post coding at both ends. We first focus on polarization precoding in this section.

Assuming full CSIT, the effective channel impulse response matrix can be decomposed by SVD as

$$H^{\text{eff}} = W \Sigma U^\dagger, \quad (5)$$

where Σ is a diagonal matrix containing singular values, and W and U^\dagger are unitary matrices composed of the left and right singular vectors, respectively [16]. In this paper, $(\cdot)^\dagger$ is the Hermitian transpose operation. The channel capacity with SVD-based precoding and postcoding is

$$C = \sum_{k=1}^{R_{H^{\text{eff}}}} \log_2 \left(1 + \frac{P_k}{\sigma_n^2} \sigma_k^2 \right), \quad (6)$$

where $R_{H^{\text{eff}}}$ is the rank of the matrix H^{eff} , and P_k is the power allocated to the k th eigenmode. Further, σ_k is the k th singular value of the effective channel impulse response matrix H^{eff} , and σ_n^2 is the noise power. Capacity maximization is achieved by a power allocation P_k that satisfies waterfilling conditions

$$P_k = \max \left(0, \epsilon - \frac{\sigma_n^2}{\sigma_k^2} \right) \text{ s.t. } P = \sum_{k=1}^{R_{H^{\text{eff}}}} P_k, \quad (7)$$

i.e., the threshold ϵ is determined by the constraint of the total transmitted power P . We assume the total power is independent of the number of antennas.

Following [17], we use Jensen's inequality to obtain

$$C \leq R_{H^{\text{eff}}} \log_2 \left(1 + \frac{1}{R_{H^{\text{eff}}}} \sum_{k=1}^{R_{H^{\text{eff}}}} \frac{P_k}{\sigma_n^2} \sigma_k^2 \right) \quad (8)$$

$$= R_{H^{\text{eff}}} \log_2 \left(\frac{1}{R_{H^{\text{eff}}}} \frac{\epsilon}{\sigma_n^2} \sum_{k=1}^{R_{H^{\text{eff}}}} \sigma_k^2 \right), \quad (9)$$

where high signal-to-noise (SNR) ratio is assumed; all P_k is greater than zero, i.e., $P_k = \epsilon - \sigma_n^2 / \sigma_k^2 > 0$ in (7). Further, σ_k^2 is the eigenvalue of $(H^{\text{eff}}(H^{\text{eff}})^\dagger)$; therefore [18],

$$\sum_{k=1}^{R_{H^{\text{eff}}}} \sigma_k^2 = \text{Tr}(H^{\text{eff}}(H^{\text{eff}})^\dagger) = \sum_{n,m} |h_{nm}^{\text{eff}}|^2. \quad (10)$$

This is the sum of squared envelopes of all channel impulse response elements in H^{eff} ; notice that each element of H^{eff} is affected by the Tx- and Rx-polarization as implied in (1). Hence, the polarization vectors at polarization-agile antenna elements impact constructively or destructively on the MIMO channel capacity even though SVD-based precoding/postcoding reaches the MIMO channel capacity for the given full CSIT.

The j th Tx polarization-agile antenna affects the j th column in (1); thus, the sum of squared singular values in (10) can be written as

$$\begin{aligned} \sum_{k=1}^{R_{H^{\text{eff}}}} \sigma_k^2 &= \sum_{j=1}^{N_t} \sum_{i=1}^{N_r} \vec{p}_{\text{Tx},j}^T \left(H_{ij}^\dagger \vec{p}_{\text{Rx},i} \vec{p}_{\text{Rx},i}^T H_{ij} \right) \vec{p}_{\text{Tx},j} \\ &= \sum_{j=1}^{N_t} \vec{p}_{\text{Tx},j}^T H_{\text{Tx},j}^{\text{PD}} \vec{p}_{\text{Tx},j}, \end{aligned} \quad (11)$$

where the “Tx-polarization-determinant matrix” for the j th Tx polarization-agile antenna, $H_{\text{Tx},j}^{\text{PD}}$, is defined as

$$H_{\text{Tx},j}^{\text{PD}} \triangleq \sum_{i=1}^{N_r} H_{ij}^\dagger \vec{p}_{\text{Rx},i} \vec{p}_{\text{Rx},i}^T H_{ij}. \quad (12)$$

The Tx-polarization vector at each Tx polarization-agile antenna is independent of those at other Tx-polarization antennas; therefore, the optimal Tx-polarization vector at the j th Tx polarization-agile antenna, $\vec{p}_{\text{Tx},j}$, is the one which maximizes $\vec{p}_{\text{Tx},j}^T H_{\text{Tx},j}^{\text{PD}} \vec{p}_{\text{Tx},j}$ in (11).

From the viewpoint of the linear-algebraic approach, $\vec{p}_{\text{Tx},j}^T H_{\text{Tx},j}^{\text{PD}} \vec{p}_{\text{Tx},j}$ is positive semi-definite; thus, the equation, $\vec{p}_{\text{Tx},j}^T H_{\text{Tx},j}^{\text{PD}} \vec{p}_{\text{Tx},j} = c_j$ corresponds to the ellipse as portrayed in Fig. 2, where x and y coordinates correspond to the elements of $\vec{p}_{\text{Tx},j}$, i.e., $p_{\text{Tx},j}^x$ and $p_{\text{Tx},j}^y$, respectively [18]. Geometrically, the principal axes of the ellipse are along eigenvectors of the matrix $H_{\text{Tx},j}^{\text{PD}}$, \vec{e}_1 and \vec{e}_2 , and the distances from the origin to the ellipse along the principal axes are $c_j / \sqrt{\lambda_1^{\text{PD}}}$ and $c_j / \sqrt{\lambda_2^{\text{PD}}}$, where λ_1^{PD} and λ_2^{PD} are the eigenvalues of $H_{\text{Tx},j}^{\text{PD}}$.

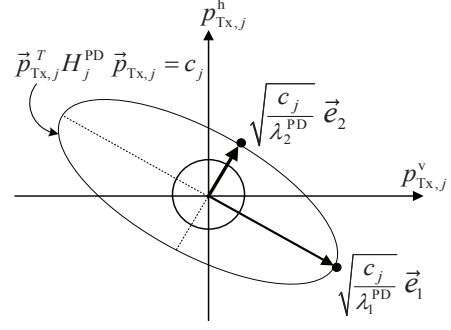


Fig. 2. Polarization-determinant ellipse and polarization-vector unit circle.

Our objective at this stage is to estimate the optimal Tx-polarization vector at each Tx polarization-agile antenna element, $\vec{p}_{\text{Tx},j} \in j = \{1, \dots, N_t\}$, which maximizes the column-sum of element-wise squared envelopes in H^{eff} , i.e., $\vec{p}_{\text{Tx},j}^T H_{\text{Tx},j}^{\text{PD}} \vec{p}_{\text{Tx},j}$. On the other hand, Tx-polarization vector $\vec{p}_{\text{Tx},j}$ is on the unit circle as presented in (3); therefore, the ellipse must have, at least, one intersection or contact point with the unit circle; whereas, at the same time it must make $\vec{p}_{\text{Tx},j}^T H_{\text{Tx},j}^{\text{PD}} \vec{p}_{\text{Tx},j} = c_j$ as large as it can. Hence, the optimal Tx-polarization vector $\vec{p}_{\text{Tx},j}^{\text{opt}}$ and corresponding optimal Tx-polarization angle θ_j^{opt} described in (3) are as

$$\vec{p}_{\text{Tx},j}^{\text{opt}} = \arg \max_{\vec{p}_{\text{Tx},j}} \vec{p}_{\text{Tx},j}^T H_{\text{Tx},j}^{\text{PD}} \vec{p}_{\text{Tx},j} = \vec{e}_2, \quad (13)$$

$$\theta_j^{\text{opt}} = \arctan(\vec{e}_2). \quad (14)$$

Notice that \vec{e}_2 is the eigenvector corresponding to λ_2 , which is the maximum eigenvalue of Tx-polarization-determinant matrix, $H_{\text{Tx},j}^{\text{PD}}$. In this manner, each Tx polarization-agile antenna element can perform polarization precoding with the optimal Tx-polarization vector.

In a completely analogous manner, the optimal RX-polarization vector can be derived; we just now have to employ the row-sum (instead of the column-sum) of element-wise squared envelopes in H^{eff} . The optimum polarization vector can be shown to be

$$\vec{p}_{\text{Rx},i}^{\text{opt}} = \arg \max_{\vec{p}_{\text{Rx},i}} \vec{p}_{\text{Rx},i}^T H_{\text{Rx},i}^{\text{PD}} \vec{p}_{\text{Rx},i} = \vec{e}_2, \quad (15)$$

$$\theta_i^{\text{opt}} = \arctan(\vec{e}_2), \quad (16)$$

where the “Rx-polarization-determinant matrix” for the i th Rx polarization-agile antenna, $H_{\text{Rx},i}^{\text{PD}}$, is defined as

$$H_{\text{Rx},i}^{\text{PD}} \triangleq \sum_{j=1}^{N_t} H_{ij} \vec{p}_{\text{Tx},j} \vec{p}_{\text{Tx},j}^T H_{ij}^\dagger. \quad (17)$$

B. Joint Polarization Pre-post Coding for Polarization Matching

The Tx-polarization-determinant matrix at the j th Tx polarization-agile antenna, $H_{\text{Tx},j}^{\text{PD}}$, depends on the Rx-polarization vectors $\vec{p}_{\text{Rx},i}$ as shown in (12), and vice versa in (17). Further, Tx- and Rx-polarization mismatching will

deteriorate the system performance in terms of the channel capacity in this paper. For those reasons, joint polarization pre-post coding is required to maximize P-MIMO channel capacity.

Since joint optimization of the pre-post coding is difficult to obtain in closed form (and also difficult to implement), we propose an iterative approach where one iteration is a sequential loop of polarization precoding; then polarization postcoding. In the k th iteration stage, $\vec{p}_{\text{Tx},j}^{\text{opt},(k-1)}$ is updated to $\vec{p}_{\text{Tx},j}^{\text{opt},(k)}$ based on $\vec{p}_{\text{Rx},i}^{\text{opt},(k-1)}$ according to (12) – (14). Then, in turn, $\vec{p}_{\text{Rx},i}^{\text{opt},(k-1)}$ is updated to $\vec{p}_{\text{Rx},i}^{\text{opt},(k)}$ based on the updated $\vec{p}_{\text{Tx},j}^{\text{opt},(k)}$ following (15) – (17). Note that while each step increases the capacity, the procedure is not guaranteed to reach the *global* optimum. However, we will see in Section IV that the capacity resulted from the iterative joint pre-post coding is in a close agreement with the one achieved by brute-force numerical search over all pre-post coding vectors.

IV. NUMERICAL EXPERIMENTS AND RESULTS

In this section we provide evaluations of our closed-form equations for optimum polarization vectors and the associated capacity. We also compare the results to brute-force numerical optimization, where we step through all possible (discretized) values of the Tx/Rx-polarization angle and choose the optimal values that corresponds to the maximum capacity for each P-MIMO channel realization. The step width of the brute-force numerical search are, respectively, 1° in Figs. 3 and 4; 5° in Figs. 5 and 6; 10° in Figs. 7 and 8. Unless stated otherwise, we consider independent and identically distributed (i.i.d.) Rayleigh fading channels with a cross-polarization discrimination, XPD = 0 dB.

We first investigate the impact of polarization agility in several deterministic channels. The P-MIMO channel capacity in a 2×2 MIMO system with polarization-agile antenna elements is portrayed for varying Tx-polarization angles in Figs. 3 and 4. The relatively low SNR regime such as 5 dB and the very high SNR regime such as 30 dB are shown in Figs. 3 and 4, respectively. In both scenarios, the channel capacity obtained by the polarization precoding at the Tx exhibits negligible difference from that yielded by the numerical result as indicated in both figures. For the 5 dB SNR in Fig. 3, the theoretically derived optimal Tx-polarization angles themselves have insignificant differences from numerically derived optimal Tx-polarization angles. In contrast, in the very high SNR regime in Fig. 4, the differences between theoretically and numerically obtained optimal Tx-polarization angles are considerable. This is due to the fact that the approximation (8) is less accurate at higher SNRs. However, the difference in capacity is still remarkably small. In case of polarization postcoding at the Rx, similar results are attained owing to the symmetry described in Sections III-A; therefore, the results are omitted here. It is worth mentioning that optimal Tx- or Rx-polarization vectors are not necessarily orthogonal, which corresponds to 90° difference in Tx- or Rx-polarization angles, as described in Figs. 3 and 4.

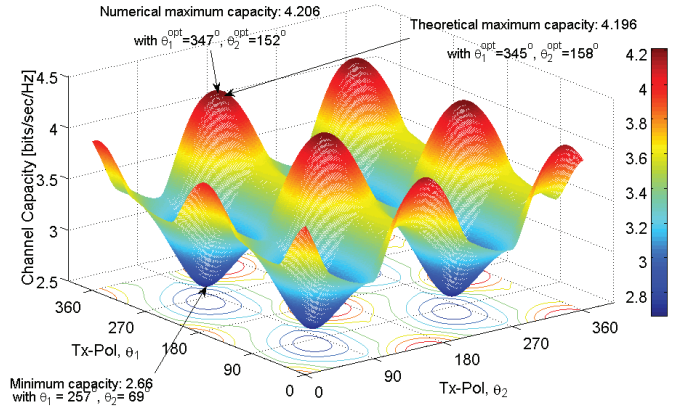


Fig. 3. Channel capacity for varying Tx-polarization; 5 dB SNR.

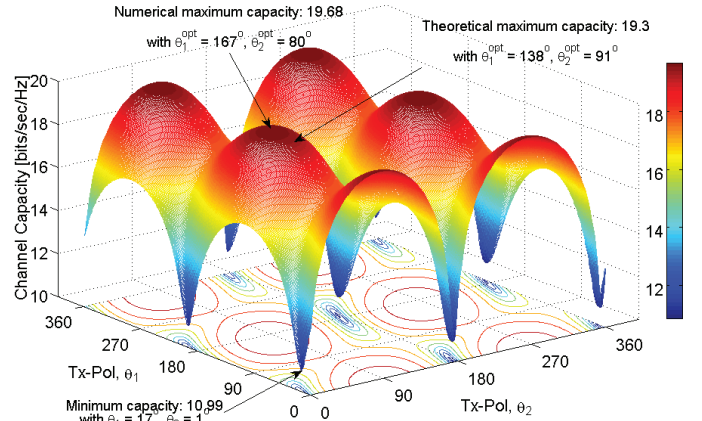


Fig. 4. Channel capacity for varying Tx-polarization; 30 dB SNR.

The P-MIMO channel capacity with the optimal Tx-polarization angles is demonstrated to depend on varying Rx-polarization angles in Fig. 5, where we also consider the 2×2 MIMO system with polarization-agile antenna elements at both ends of the Tx and the Rx. The channel capacity exhibits substantial variation from 21.47 bits/sec/Hz to 13.60 bits/sec/Hz depending on Rx-polarization angles, although Tx-polarization angles are already set to the optimum obtained by brute-force numerical search as will be shown in Fig. 6, i.e., $\theta_{\text{Tx}-1} = 80^\circ$; $\theta_{\text{Tx}-2} = 50^\circ$. This result obviously shows that the polarization mismatching between the Tx and the Rx can cause significant deterioration in the capacity of the whole system, even if one end of the Tx and the Rx is already set to the optimal polarization. However, the proposed scheme of joint polarization pre-post coding also shows negligible difference from numerical results in both optimal Tx- and Rx-polarization angles and channel capacity.

Local optimal Tx- and Rx-polarization vectors at each iteration of joint polarization pre-post coding are depicted in Fig. 6 considering the same scenario of channel impulse matrices and SNR as that in Fig. 5. The 2×2 P-MIMO system is again considered in this figure. Here, one iteration is a sequential loop of polarization precoding and then polarization postcoding as described in Section III-B. Tx/Rx-polarization

vectors quickly converge; moreover, these global optimal polarization vectors show relatively small difference from the numerical optimum.

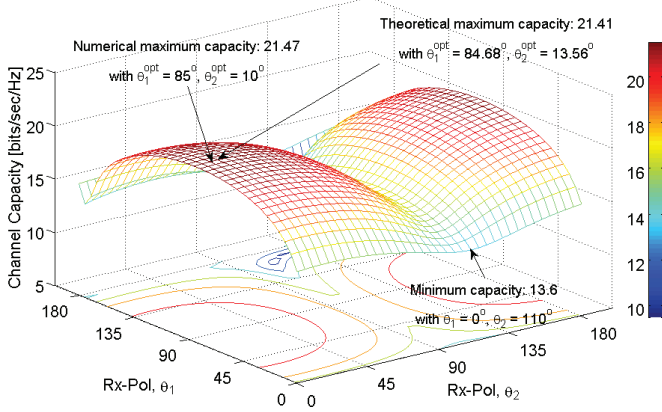


Fig. 5. Channel capacity for varying Rx-polarization with optimal Tx-polarization; 30 dB SNR.

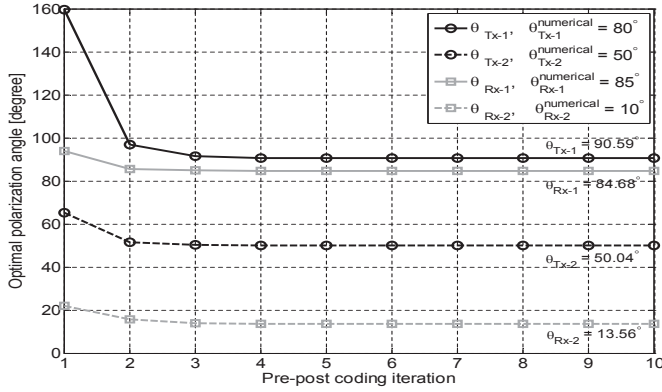


Fig. 6. Optimal Tx/Rx-polarization angles for the number of iterations; 30 dB.

In contrast to Figs. 3 – 6, from this point on, we investigate how much the joint polarization pre-post coding improves the P-MIMO channel capacity in a statistical sense in Figs. 7 – 9. The simulation results are based on the 10^4 times realizations of i.i.d. Rayleigh fading channels. Figures 7 and 8 depict cumulative density functions (cdf's) of the 2×2 P-MIMO channel capacity at 5 dB SNR and 30 dB SNR, respectively, for the scenarios of joint polarization pre-post coding with Tx/Rx polarization-agile antennas; and random Tx/Rx-polarization. It is noteworthy that the cdf resulted from the fixed Tx/Rx-polarization exhibits exactly the same cdf of random Tx/Rx-polarization at each channel realization owing to the random generation of the i.i.d. Rayleigh fading channels. Furthermore, the cdf's of the optimal and the worst Tx/Rx-polarization obtained by brute-force numerical search at each channel realization, are presented in Figs. 7 and 8. We perform five iterations for the joint polarization pre-post coding at each P-MIMO channel realization, which results in the satisfactory convergence of Tx/Rx-polarization vectors on the global optimal ones as demonstrated in Fig. 6.

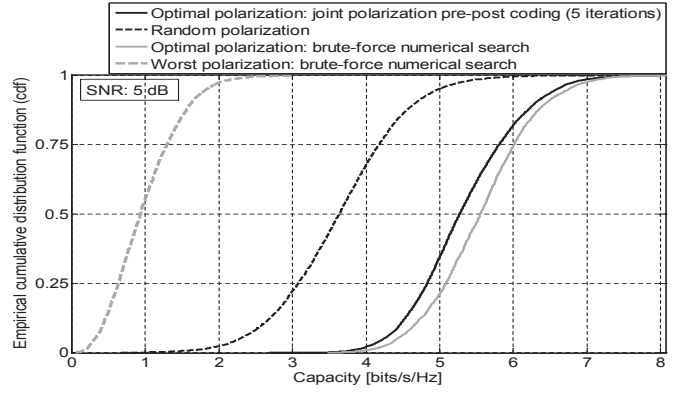


Fig. 7. cdf's of channel capacity for the scenarios of joint polarization pre-post coding with five iterations, random Tx/Rx-polarization; optimal and the worst Tx/Rx-polarization through brute-force numerical search at 5 dB SNR.

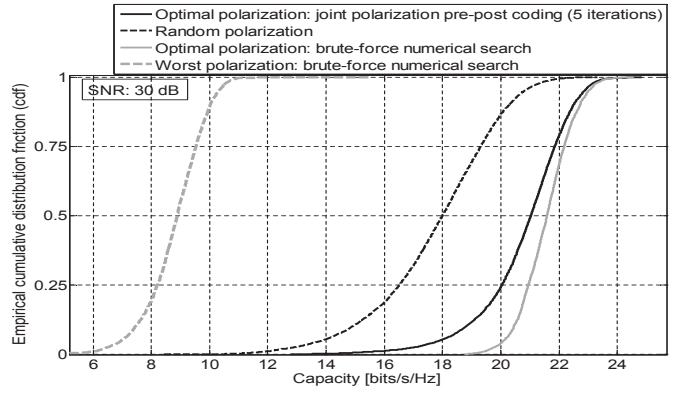


Fig. 8. cdf's of channel capacity for the scenarios of joint polarization pre-post coding with five iterations, random Tx/Rx-polarization; optimal and the worst Tx/Rx-polarization through brute-force numerical search at 30 dB SNR.

Our joint polarization pre-post coding significantly improves the P-MIMO channel capacity at both 5 dB SNR and 30 dB SNR. In Fig. 7, the probability of the P-MIMO channel capacity less than 4.2 bits/sec/Hz is 0.75 with 5 dB SNR and random Tx/Rx-polarization; whereas, with the proposed joint polarization pre-post coding, the probability of the capacity greater than 4.2 bits/sec/Hz is 0.94. For the improvement of the P-MIMO channel capacity at 30 dB SNR in Fig. 8, the probability of the capacity greater than 20 bits/sec/Hz is 0.75 in the scenario of utilizing joint polarization pre-post coding, while that probability is just 0.12 with random Tx/Rx-polarization. It is noteworthy that the cdf curves of random Tx/Rx-polarization scenarios in both Figs. 7 and 8 can be regarded as the expectation of the cdf curves in a statistical sense when the joint polarization pre-post coding is not utilized; however, the practical channel capacity would exhibit substantial variations between the cdf curves associated with the optimal and the worst Tx/Rx-polarization obtained by brute-force numerical search in both figures.

The joint polarization pre-post coding achieves significant improvement of P-MIMO channel capacity so that its cdf curve remarkably approaches the best cdf curve obtained by

brute-force numerical search, in particular, at 5 dB SNR in Fig. 7. The cdf curve corresponding to the proposed scheme also exhibits slight difference from the best cdf curve resulted from brute-force numerical search at the 30 dB SNR in Fig. 8, comparing to the significant difference between that best-scenario cdf and the cdf of random Tx/Rx-polarization or, more seriously, between the best- and the worst-scenario cdf's obtained by the numerical search.

Finally, we compare channel capacity for varying SNR and the varying number of polarization-agile antennas in Fig. 9. For each setting of the number of polarization-agile antennas, Fig. 9 demonstrates three scenarios: joint polarization pre-post coding at both link ends; Tx-polarization precoding only at the transmitter; and random Tx/Rx-polarization as the baseline control. In the high SNR regime, utilizing our joint polarization pre-post coding remarkably improves P-MIMO channel capacity with around 5 dB, 4 dB, and 3dB SNR gains in the cases of 2×2 , 3×3 , and 4×4 P-MIMO channels, respectively.

Moreover, it is noteworthy that in a relatively low SNR regime below 9 dB, 2×2 and 3×3 P-MIMO systems adopting the proposed joint polarization pre-post coding accomplish almost the same channel capacity as, respectively, 3×3 and 4×4 MIMO systems with random Tx/Rx-polarization. We also note that the P-MIMO system with our joint polarization pre-post coding shows better channel capacity even than the P-MIMO system that has one more antenna element at both link ends of the transmitter and receiver and uses random polarization, in the low SNR regime below 3 dB.

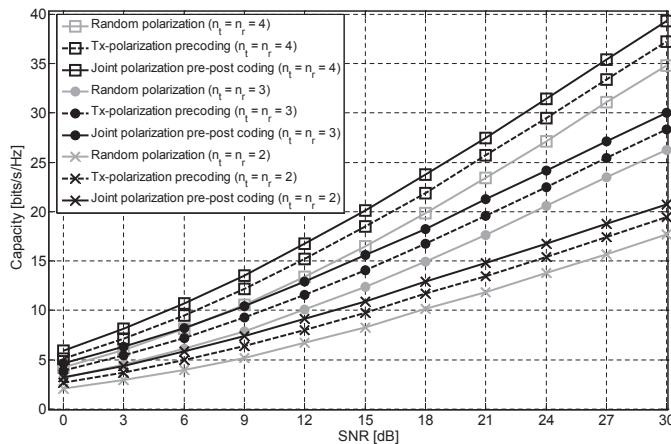


Fig. 9. P-MIMO channel capacity for the varying SNR in the scenarios of random Tx/Rx-polarization, Tx-polarization precoding, and joint polarization pre-post coding.

V. CONCLUSION

In this paper, we proposed the use of polarization-agile antennas as a means to improve capacity of MIMO systems without requiring increased number of RF chains. Adjustment of the polarization angles of those antennas to the instantaneous channel state was shown to significantly improve capacity. For the case of polarization-agile antennas at one

link end, we derived in closed-form (approximately) optimal polarization vectors and showed that their performance closely approaches that of the true global optimum obtained through brute-force numerical search. In the proposed joint polarization pre-post coding, the local optimum usually reaches the global optimum of Tx/Rx-polarization vectors within five iterations at both high and low SNR. The proposed method offers an alternative, low-cost and low-energy-consumption method for capacity increase in MIMO systems.

ACKNOWLEDGMENT

Part of this work was supported financially by the National Science Foundation.

REFERENCES

- [1] R. G. Vaughan, "Polarization diversity in mobile communications," *IEEE Trans. Veh. Technol.*, vol. 39, no. 3, pp. 177–185, Jun. 1990.
- [2] V. Erceg, P. Soma, D. Baum, and S. Catreux, "Multiple-input multiple-output fixed wireless radio channel measurements and modeling using dual-polarized antennas at 2.5 GHz," *IEEE Trans. Wireless Commun.*, vol. 3, no. 6, pp. 2288 – 2298, Nov. 2004.
- [3] M. Shafi, M. Zhang, A. Moustakas, P. Smith, A. Molisch, F. Tufvesson, and S. Simon, "Polarized MIMO channels in 3-D: Models, measurements, and mutual information," *IEEE J. Sel. Areas Commun.*, vol. 24, no. 3, pp. 514–527, Mar. 2006.
- [4] S.-C. Kwon, "Geometrical theory, modeling and applications of channel polarization," *Ph.D. Thesis, Georgia Institute of Technology*, pp. 1–128, 2014.
- [5] S.-C. Kwon and G. L. Stüber, "Geometrical theory of channel depolarization," *IEEE Trans. Veh. Technol.*, vol. 60, no. 8, pp. 3542–3556, Oct. 2011.
- [6] S.-C. Kwon, G. Stüber, A. López, and J. Papapolymou, "Geometrically based statistical model for polarized body-area-network channels," *IEEE Trans. Veh. Technol.*, vol. 62, no. 8, pp. 3518–3530, Oct. 2013.
- [7] R. Nabar, H. Bolcskei, V. Erceg, D. Gesbert, and A. Paulraj, "Performance of multiantenna signaling techniques in the presence of polarization diversity," *IEEE Trans. Sig. Proc.*, vol. 50, no. 10, pp. 2553–2562, Oct. 2002.
- [8] Y. Deng, A. Burr, and G. White, "Performance of MIMO systems with combined polarization multiplexing and transmit diversity," in *Proc. IEEE Veh. Technol. Conf.*, vol. 2, May 2005, pp. 869–873.
- [9] J. Jootar, J.-F. Diouris, and J. Zeidler, "Performance of polarization diversity in correlated Nakagami-m fading channels," *IEEE Transactions on Vehicular Technology*, vol. 55, no. 1, pp. 128–136, 2006.
- [10] H. Nishimoto, A. Taira, H. Kubo, M. O. Pun, R. Annavajjala, and A. Molisch, "Performance evaluation of cross-polarized antenna selection over 2 GHz measurement-based channel models," in *IEEE Vehicular Technology Conference*, 2011, pp. 1–5.
- [11] S.-C. Kwon, "Optimal power and polarization for the capacity of polarization division multiple access channels," in *Proc. IEEE Global Telecommun. Conf.*, Dec. 2014, pp. 1–5.
- [12] S.-C. Kwon and G. Stüber, "Polarization division multiple access on NLoS wide-band wireless fading channels," *IEEE Trans. Wireless Commun.*, vol. 13, no. 7, pp. 3726–3737, Jul. 2014.
- [13] D. Landon and C. Furse, "Recovering handset diversity and MIMO capacity with polarization-agile antennas," *IEEE Trans. Antennas Propag.*, vol. 55, no. 11, pp. 3333–3340, Nov 2007.
- [14] O. Karabey, S. Bildik, S. Bausch, S. Strunck, A. Gaebler, and R. Jakob, "Continuously polarization agile antenna by using liquid crystal-based tunable variable delay lines," *IEEE Trans. Antennas Propag.*, vol. 61, no. 1, pp. 70–76, Jan 2013.
- [15] A. Molisch and M. Win, "MIMO systems with antenna selection," *IEEE Microwave Magazine*, vol. 5, no. 1, pp. 46–56, Mar 2004.
- [16] A. F. Molisch, *Wireless Communications*, 2nd ed. Wiley and IEEE, 2010.
- [17] D. Tse and P. Viswanath, *Fundamentals of Wireless Communication*, 1st ed. Cambridge, 2005.
- [18] G. Strang, *Linear Algebra and Its Applications*, 4th ed. Thomson Learning, Inc., 2005.